ORIGINAL RESEARCH

Alternative Oxidase Attenuates Cigarette Smoke–induced Lung Dysfunction and Tissue Damage

Luca Giordano[1,2,3,4], Antoine Farnham[1,2], Praveen K. Dhandapani[1,2], Laura Salminen[1,2], Jahnavi Bhaskaran[1,2], Robert Voswinckel[5], Peter Rauschkolb[3,4], Susan Scheibe[3,4], Natascha Sommer[3,4], Christoph Beisswenger[6], Norbert Weissmann[3,4], Thomas Braun[7], Howard T. Jacobs[1,2], Robert Bals[6], Christian Herr[6*], and Marten Szibor[1,2,7*]

[1]Faculty of Medicine and Life Sciences, University of Tampere, Tampere, Finland; [2]Institute of Biotechnology, University of Helsinki, Helsinki, Finland; [3]Excellence Cluster Cardio-Pulmonary System, University of Giessen, Giessen, Germany; [4]Marburg Lung Center, Member of the German Center for Lung Research, Justus Liebig University, Giessen, Germany; [5]Bürgerhospital Friedberg, Klinik für Innere Medizin, Friedberg, Germany; [6]Department of Internal Medicine V–Pulmonology, Allergology, Intensive Care Medicine, Saarland University, Homburg/Saar, Germany; and [7]Department I Cardiac Development and Remodeling, Max Planck Institute for Heart and Lung Research, Bad Nauheim, Germany

ORCID IDs: 0000-0001-6315-7361 (L.G.); 0000-0001-9422-6569 (C.H.); 0000-0003-4029-160X (M.S.).

Abstract

Cigarette smoke (CS) exposure is the predominant risk factor for the development of chronic obstructive pulmonary disease (COPD) and the third leading cause of death worldwide. We aimed to elucidate whether mitochondrial respiratory inhibition and oxidative stress are triggers in its etiology. In different models of CS exposure, we investigated the effect on lung remodeling and cell signaling of restoring mitochondrial respiratory electron flow using alternative oxidase (AOX), which bypasses the cytochrome segment of the respiratory chain. AOX attenuated CS-induced lung tissue destruction and loss of function in mice exposed chronically to CS for 9 months. It preserved the cell viability of isolated mouse embryonic fibroblasts treated with CS condensate, limited the induction of apoptosis, and decreased the production of reactive oxygen species (ROS). In contrast, the early-phase inflammatory response induced by acute CS exposure of mouse lung, i.e., infiltration by macrophages and neutrophils and adverse signaling, was unaffected. The use of AOX allowed us to obtain novel pathomechanistic insights into CS-induced cell damage, mitochondrial ROS production, and lung remodeling. Our findings implicate mitochondrial respiratory inhibition as a key pathogenic mechanism of CS toxicity in the lung. We propose AOX as a novel tool to study CS-related lung remodeling and potentially to counteract CS-induced ROS production and cell damage.

Keywords: cigarette smoke; COPD; mitochondria; alternative oxidase

Clinical Relevance

Cigarette smoke exposure triggers mitochondrial respiratory inhibition and oxidative stress. The use of an alternative respiratory enzyme relieves mitochondrial stress and attenuates lung dysfunction and tissue damage.

Chronic obstructive pulmonary disease (COPD), which is largely caused by exposure to cigarette smoke (CS), represents a rapidly growing global health burden in terms of suffering and mortality. It is estimated that it will soon become the third most common cause of death worldwide (1). The clinical hallmarks of COPD are airflow limitations and lung tissue destruction. The poor regeneration capacity of the adult human lung and the lack of therapeutic interventions to arrest or reverse tissue

destruction make COPD a terminal condition. Different possible mechanisms driving the pathology of this disease are currently the subject of intense debate and experimentation. It has been proposed, for instance, that local inflammation and production of reactive oxygen species (ROS) induced upon CS exposure initiate adverse lung remodeling (2). The prooxidant nature of CS is well documented and supports this hypothesis (3). However, its complex composition, which includes more than 5,000 compounds (4), many of which are known toxins or carcinogens, complicates efforts to elucidate the underlying mechanism. Two prominent CS compounds are known as potent inhibitors of mitochondrial respiratory complex IV (cIV), i.e., carbon monoxide and hydrogen cyanide. Exposure to either toxin disrupts electron transport, inducing cellular redox imbalance and excessive ROS production. Because cyanide has a systemic half-life of up to 25 hours (5), mitochondrial impairment cannot be considered as an inert bystander in the development of COPD. Instead, excess ROS produced as a result of respiratory chain inhibition may be the actual trigger for adverse signaling that initiates and accelerates the pathology.

Plants and many lower organisms, including the sea-squirt *Ciona intestinalis*, but not mammals, express alternative oxidase (AOX), which is able to maintain mitochondrial respiration under conditions in which the cytochrome segment of the electron transport chain is blocked. Specifically, AOX accepts electrons from ubiquinol to reduce oxygen to water. Notably, because AOX is a single-subunit oxidase and nonproton pumping, it does not add to the proton motive force across the inner mitochondrial membrane and thus does not directly support mitochondrial ATP production. Recently, we engineered and characterized mouse models that ubiquitously expressed AOX (6, 7). Even globally expressed AOX caused no deviation from normal physiology, including body temperature and regular mitochondrial oxygen consumption, while conferring resistance to respiratory chain inhibitors such as antimycin A and cyanide (6, 7). This seemingly counterintuitive outcome can be explained by the biochemical properties of AOX, which requires respiratory disruption and sufficient Q-pool reduction for proper functioning (8). This makes AOX an ideal tool for studying mitochondrial

involvement in pathogenesis in the mouse (9, 10). For example, the use of AOX mice in a disease model for sepsis revealed that mitochondria are responsible for the detrimental proinflammatory phenotype shift of macrophages, and, more importantly, that transgenic expression of AOX decreases lethality by restoring mitochondrial respiration and blunting the production of mitochondrial ROS in bone marrow–derived macrophages (11). Our previous data indicate that AOX is sufficiently active in immune cells, which are also responsible for the local inflammation and excess ROS production seen in the course of COPD (11). Thus, we sought to test whether CS-induced respiratory inhibition could be revoked by AOX and whether this would decrease ROS production, alleviating cell damage and limiting immune cell migration to the lung and adverse organ remodeling *in vivo*.

Here, we show in AOX mice chronically exposed to CS that detrimental lung remodeling is attenuated while functional lung parameters (lung mechanics) are preserved. At the cellular level, AOX protects against the toxicity of CS condensate (CSC), decreasing mitochondrial superoxide production and preserving cell viability. In contrast, the acute response to short-term CS exposure, i.e., the infiltration of neutrophils and macrophages, is not prevented by AOX, suggesting that the relationship between the early inflammatory response and long-term lung remodeling is not straightforward. We infer that the early- and late-phase responses must differ, with mitochondrial signaling being sufficient to account only for the latter. Nevertheless, the use of AOX provides novel insights into disease etiologies and may form the basis for novel approaches to counteract the development of chronic lung remodeling, such as that seen in COPD.

Methods

Animal Experiments
A mouse strain ubiquitously expressing AOX was recently described (6). All animal experiments were approved by the Landesamt für Soziales, Gesundheit und Verbraucherschutz, of the State of Saarland following the national guidelines for animal treatment (18/2011), and were performed according to the Declaration of Helsinki conventions for the use and care of animals.

CS Exposure
Female heterozygous AOX transgenic mice and wild-type (WT) littermates were exposed to CS (3R4F cigarettes, College of Agriculture, Reference Cigarette Program, University of Kentucky) in a TE-10 smoking machine (Teague Enterprises) starting at 8 weeks of age (12, 13).

Lung Function Measurements
Respiratory system mechanics were analyzed using the flexiVent system (SCIREQ) as previously described (12, 14).

Stereological Lung-Tissue Analysis
Lungs were fixed by instillation of PBS-buffered 4% formaldehyde in PBS under constant hydrostatic pressure, prepared by systematic uniform random sampling, and analyzed as previously described (12, 13).

BAL
Animals were anesthetized as described above and tracheotomized. BAL was performed as previously described (12, 13). A minimum of 200 cells were counted and differentiated based on morphology.

Quantification of Inflammatory Mediators
Concentrations of IL-6 (DY406), KC (keratinocyte derived cytokine, CXCL1) (DY453), MIP2 (macrophage inflammatory protein) (DY452), and MMP9 (matrix metalloprotease 9) (DY6718) were measured by ELISA (DuoSet; R&D Systems) according to the manufacturer's instructions. Signals were quantified using a FLUOstar Omega ELISA reader and MARS data analysis software V3.10.R6 (both from BMG Labtech).

Isolating Primary Mouse Embryonic Fibroblasts
Primary mouse embryonic fibroblasts (MEFs) from embryos at embryonic day 13.5 (E13.5)–E15.5 were isolated and immortalized (generating iMEFs) as described elsewhere (15, 16).

Generation of CSC
CSC was obtained from Vectis s.r.l. Cava dei Tirreni as the solid fraction derived from tobacco smoke and thus devoid of volatile components such as carbon monoxide (17).

Sulforhodamine B Viability Assay
Toxicity screening was conducted using the sulforhodamine B (SRB) assay (S1402; Sigma-Aldrich), which is based on measurement of cellular protein content (18).

Respirometry

Mitochondrial respiration of permeabilized cells was assayed using a respirometer (OROBOROS) as previously described (19).

ROS Measurements

The amount of ROS in iMEFs was measured using MitoSOX Red (M36008; Thermo-Fisher Scientific) and the electron-spin-resonance method as described in detail elsewhere (20, 21).

Statistics

The sample size for each experiment is stated in the figures, with all data shown as mean $\pm$ SEM or box-and-whiskers plots (SRB viability assay). Statistical analysis was performed with GraphPad Prism software (GraphPad Software Inc.). Differences were considered statistically significant at a P value of <0.05.

Results

AOX Attenuates Chronic CS-induced Lung Dysfunction and Tissue Damage

To test whether mitochondrial respiratory inhibition could be the trigger for lung damage and remodeling driven by chronic CS exposure, we subjected WT and AOX mice to chronic CS for 9 months. CS stress caused a loss of body weight in all of the exposed mice, although significance was reached only in WT animals (Figure 1A). To eliminate a possible bias by differences in body weight, all measured functional lung parameters were normalized to the actual body weight. Respiratory-system mechanics related to CS-induced lung remodeling showed a significant deterioration in WT mice (Figures 1B–1E; Figure E1A in the data supplement). In AOX mice, the loss of lung function was generally less severe or absent (Figures 1B–1E). Compared with WT controls, AOX mice were significantly protected from the effects of CS exposure as determined by volume (Figure 1B) and hysteresis (Figure 1D), whereas other parameters only showed a trend toward protection (Figures 1C and 1E). Parameters typically altered in restrictive airway diseases were unaffected by both CS exposure and AOX expression (Figures E1B–E1E).

To visualize the severity of lung damage upon chronic exposure to CS, we quantified the mean chord length by stereology (Figure 2). Again, we found an increase in
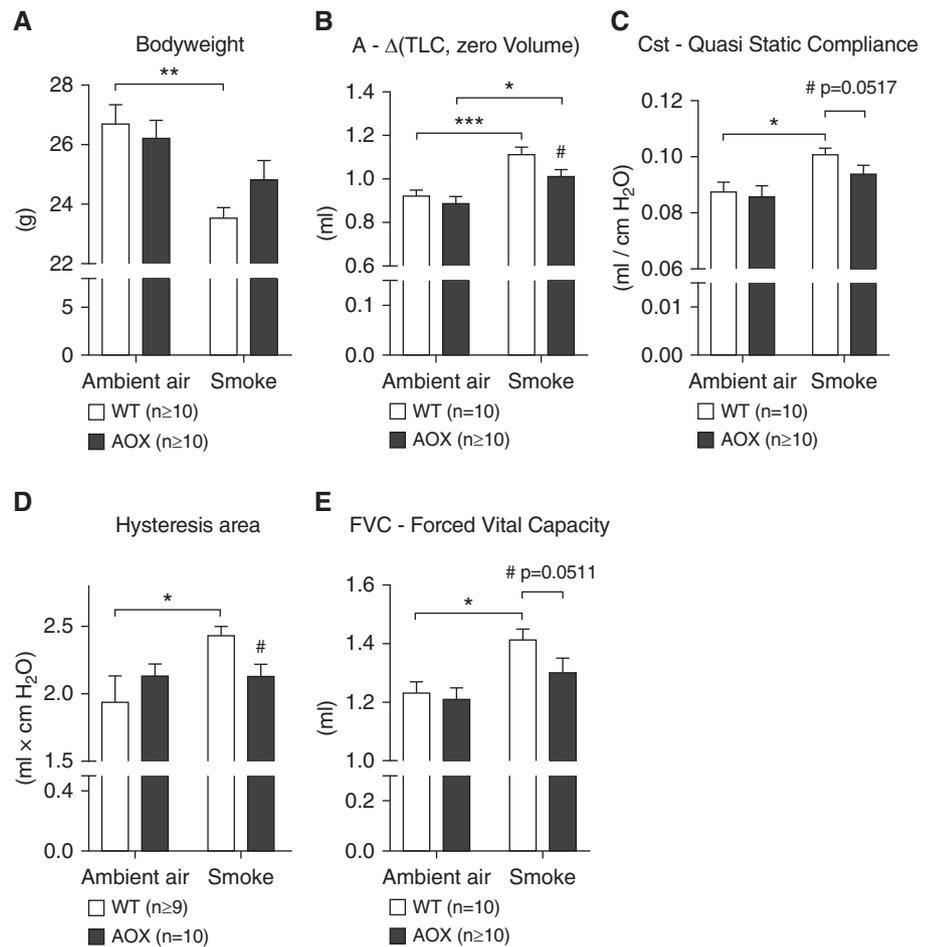

Figure 1. Effect of chronic cigarette smoke (CS) exposure on lung function in wild-type (WT) and alternative oxidase (AOX) mice. (A) Body weight of WT and AOX mice after smoke exposure. (B–E) Respiratory system mechanics measured using the SCIREQ FlexiVent system. All data are shown as mean $\pm$ SEM; $*P < 0.05$, $**P < 0.005$, and $***P < 0.0005$ by two-way ANOVA; if not stated otherwise, $^{\#}P < 0.05$ by paired t test on CS-exposed groups.

CS-exposed mice, corresponding to the observed changes in alveoli volume (Figure 2B), which were less pronounced in the CS-exposed AOX group. Taken together, these results show that AOX attenuates tissue destruction upon CS exposure.

AOX Improves Cell Viability upon CSC Exposure

To identify molecular mechanisms underlying the observed effects of AOX upon CS exposure, we used a cell-culture model. Because the strongest effects seen *in vivo* affected parameters reflecting the lung's ability to stretch and expand, such as hysteresis, we chose fibroblasts (iMEFs) as the most suitable cell type to study. Growing cells were treated with CSC and the number of viable cells after 2 or 3 days was determined using the SRB assay

(Figure 3). CSC decreased SRB staining in both WT and AOX iMEFs in a dose-dependent manner (Figures 3A and 3B). AOX conferred robust protection against CSC toxicity to cells grown in glucose (Figures 3A and 3B) or in galactose (Figures 3C and 3D), which enforces the use of mitochondrial oxidative phosphorylation (22), and where CSC had a more dramatic effect. When CSC-containing galactose medium was replaced with toxin-free medium after 48 hours, AOX-expressing, but not WT, iMEFs were able to recover (Figure 3C). Cleaved caspase-3 (Figures 3D and 3E) was significantly increased in WT, but not AOX, iMEFs after CSC exposure, whereas total caspase-3 was unaffected (Figure E2). This is consistent with the idea that CSC activates apoptosis as a result of mitochondrial respiratory inhibition, against which AOX affords protection.

4C/FPO
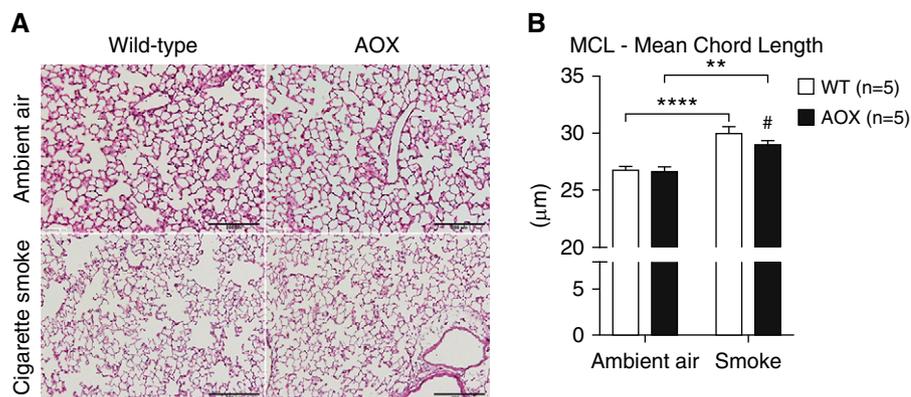
Figure 2. Stereological analysis of lung tissue. (*A*) Representative tissue slices (hematoxylin and eosin stained). (*B*) Statistical analysis of mean chord length (MCL). All data are shown as mean ± SEM; **$P < 0.005$ and ****$P < 0.0001$ by two-way ANOVA; #$P < 0.05$ by paired *t* test on smoke-exposed groups. Scale bars: 200 μm.

AOX Supports Mitochondrial Respiration and Decreases Superoxide Production in iMEFs Exposed to CSC

We used respirometry to analyze the effects of CSC on mitochondrial respiration, and how this is modified by AOX expression. Two different assays were implemented to analyze damage-associated effects of CSC on respiration and to profile any acute toxic effects of CSC on respiration. Intact iMEFs cultured in galactose medium in the presence of CSC for 48 hours showed a dose-dependent drop in respiration with partial protection by AOX at low CSC concentration (Figure E3A). To identify the specific sites of CSC-induced damage and its mitigation by AOX, we used digitonin-permeabilized cells supplied with specific substrate mixes and inhibitors. Culturing of cells in CSC resulted in a dose-dependent decrease in respiration driven by a complex I (cI)-linked substrate mix (Figure 4A), which was not compensated for by AOX expression. In contrast, AOX was able to maintain or increase respiration driven by the complex II (cII) substrate succinate, even at high doses of CSC (Figure 4B). AOX was unable to prevent the large decrease in complex IV (cIV)-driven respiration produced by a high dose of CSC, although it stimulated cIV-driven respiration at a lower (noninhibitory) dose (Figure 4C). These effects were not reflected by altered levels of representative protein subunits of the respiratory chain complexes (Figure 4D), and therefore were likely due to post-translational modifications, small-molecule effectors, or damage to prosthetic groups, e.g., brought about by ROS.

Because enhanced ROS production is a well-characterized effect of respiratory chain inhibition, specifically at the levels of cIII and cIV, we measured mitochondrial superoxide accumulation using two different methods in glucose-cultured iMEFs: MitoSOX Red staining and electron spin resonance (Figures 4E, 4F, E3B, and E3C). With either method, superoxide levels increased dramatically in iMEFs exposed to CSC for 3 hours, whereas AOX limited or prevented this induction.

Intact cell respiration was unaffected by acute exposure to CSC (Figure E4A) unless the cells were first treated with an uncoupling agent such as FCCP (carbonyl cyanide 4-[trifluoromethoxy] phenylhydrazone), revealing a dose-dependent decrease in respiratory capacity that was again mitigated by AOX (Figure E4B). In permeabilized cells, CSC inhibited respiration driven by cI- or cII-linked substrates (Figures E4C and E4D), but AOX was able to limit only the latter. cIV-driven respiration was unaffected by AOX or by CSC (Figure E4E).

AOX Has No Effect on Acute CS-induced Inflammation

Because AOX had protective effects on the outcome of chronic CS exposure *in vivo* and limited CSC-induced cell death, we reasoned that it may also prevent what is considered to be the earliest step in COPD development, i.e., CS-induced pulmonary inflammation. To test this assumption, we used a previously validated model of the acute inflammatory response to short-term CS exposure (12). This model is mainly based

on neutrophilic inflammation, mimicking conditions seen in patients. Surprisingly, we found that both macrophages and neutrophils were increased to the same degree in the BAL of WT and AOX mice (Figures 5A–5C).

Because we have shown previously that AOX expression prevents proinflammatory activation in a mouse sepsis model (11), we tested whether AOX would also prevent the adverse CS-induced inflammatory signaling response in the BAL fluid. Specifically, we quantified the presence of KC, a mouse-specific functional homolog of human IL-8, which typically correlates with the severity of COPD (23); MIP2, which together with KC belongs to the class of CXC chemokines known to induce neutrophil chemotaxis (24, 25); IL-6, which is a typical inflammatory marker that is often elevated during COPD; and MMP-9, which is activated by acrolein (26) or neutrophil elastase (27) and is known to contribute to tissue remodeling in patients with COPD during disease exacerbation (28). All of the markers were significantly and comparably upregulated in WT and AOX mice (Figures 5D–5G), indicating that AOX does not confer any protection, and suggesting that the acute-phase tissue response is not based on mitochondrial respiratory impairment.

Discussion

Our results identify impaired mitochondrial respiration as a molecular mechanism that drives lung remodeling upon CS exposure. Here, we show that a respiratory bypass can increase cell viability and, as a consequence, maintain lung function and/or facilitate repair processes. This is of significance for a number of reasons. Notably, the adult human lung lacks proper regeneration capacity. Therefore, any mechanism that attenuates the pathology is of great interest not only for millions of cigarette abusers but also for the even larger population that is exposed to toxic smoke in the environment due to urban air pollution or in a domestic setting.

By using AOX, we were able to demonstrate the involvement of mitochondria in the pathogenesis of COPD resulting from smoke exposure, and reveal relevant mechanisms underlying the effects of CS on mitochondrial respiration. For instance, we showed that CSC affects individual respiratory complexes differently.
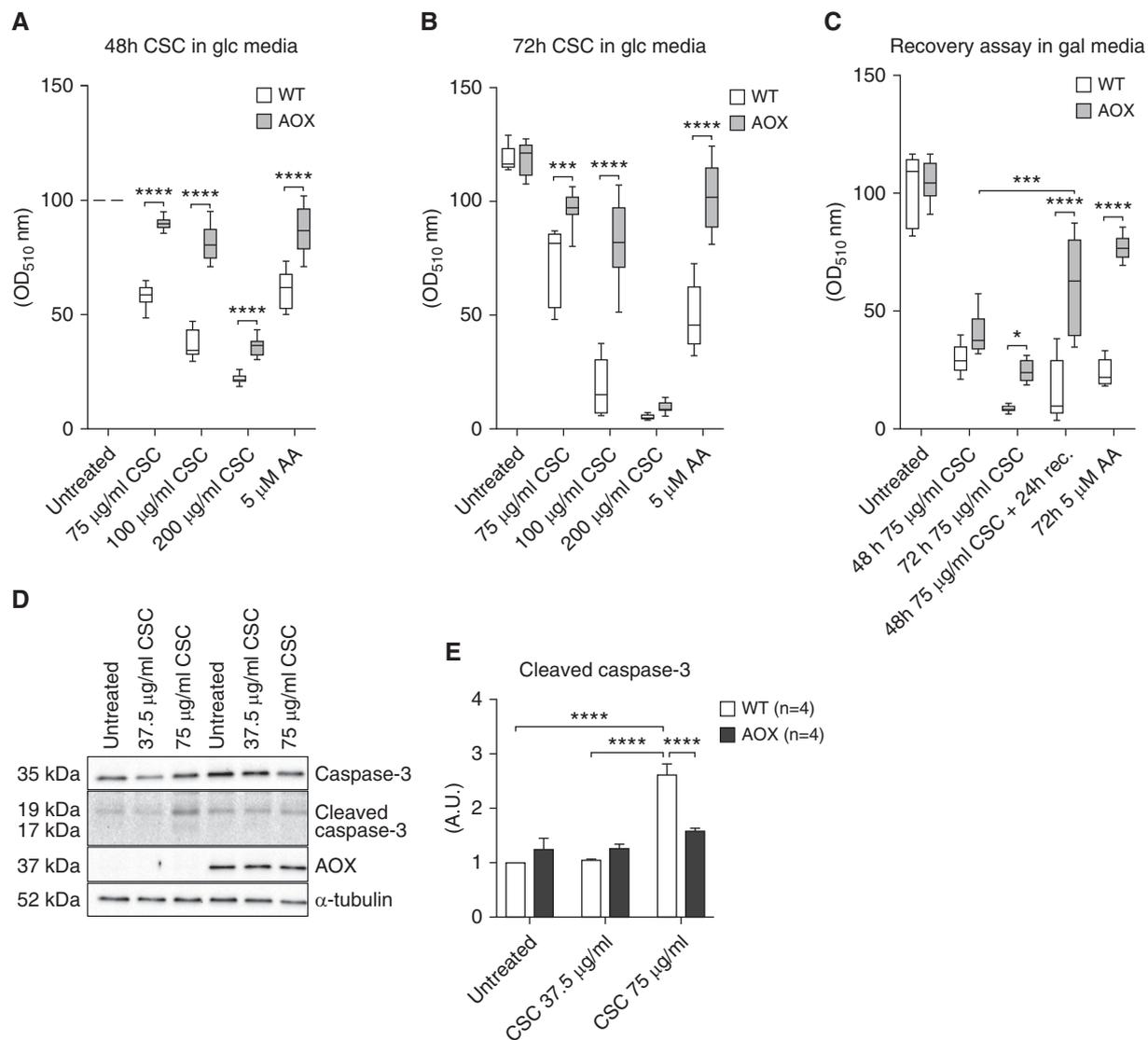
Figure 3. Analysis of CS condensate (CSC) toxicity in cultured immortalized mouse embryonic fibroblasts (iMEFs). (*A–C*) WT and AOX-expressing iMEFs cultured in glucose (glc, 10 mM) or galactose (gal, 10 mM) media and treated with CSC as indicated. Numbers of viable cells were estimated using the sulforhodamine B assay (absorbance at OD_{510}) and normalized against the value at 48 hours for untreated cells on the given medium (shown in %). In *C*, cells recovered for 24 hours in gal (10 mM) without CSC as indicated after CSC (75 μg/ml) exposure. Horizontal bands inside the boxes represent the median (second quartile), the bottom and top of the box are the first and third quartiles, respectively, and the ends of the whiskers represent the minimum and maximum values of the data set. (*D*) Western blot of caspase-3, cleaved caspase-3, and AOX, with α-tubulin as the loading control. For entire blots, including molecular-weight markers for cropped Western blot bands, please refer to Figure E5. (*E*) Relative densitometric analysis ($n \geq 3$) on proteins extracted from WT and AOX iMEFs exposed to CSC as indicated in gal media. Bar graph represents mean ± SEM; *$P < 0.05$, ***$P < 0.0005$, and ****$P < 0.0001$ by two-way ANOVA. AA = antimycin A; OD = optical density.

Although cI was inhibited both directly and indirectly upon acute and chronic (48 h) exposure, cII and cIV showed only a mild response to acute CSC exposure (Figures 4, E3, and E4). Of note, due to its mode of action, AOX cannot rescue a cI impairment, as the Q-pool will likely remain oxidized, whereas inhibition of cIII or cIV causes a Q-pool reduction. Moreover, the cII substrate succinate is known to highly reduce the Q-pool, thereby inducing reverse electron transport and thus mitochondrial ROS production when no cI inhibitor is added. Yet, the mechanisms underlying the observed activation of respiratory complexes remain to be elucidated. Although cII-driven respiration in the presence of AOX can overcome inhibition of cIII and/or cIV, the reason for the observed cII and cIV activation (Figures 4B and 4C) is unclear. One plausible explanation is that AOX prevents excessive ROS production (6, 11), as shown directly in the case of CSC exposure (Figures 4E, 4F, E3B, and E3C), and thus may prevent unspecific damage to mitochondrial and cellular components. In support of our findings, it has previously been shown that CSC inhibits the activity of respiratory complexes (17) and causes cell
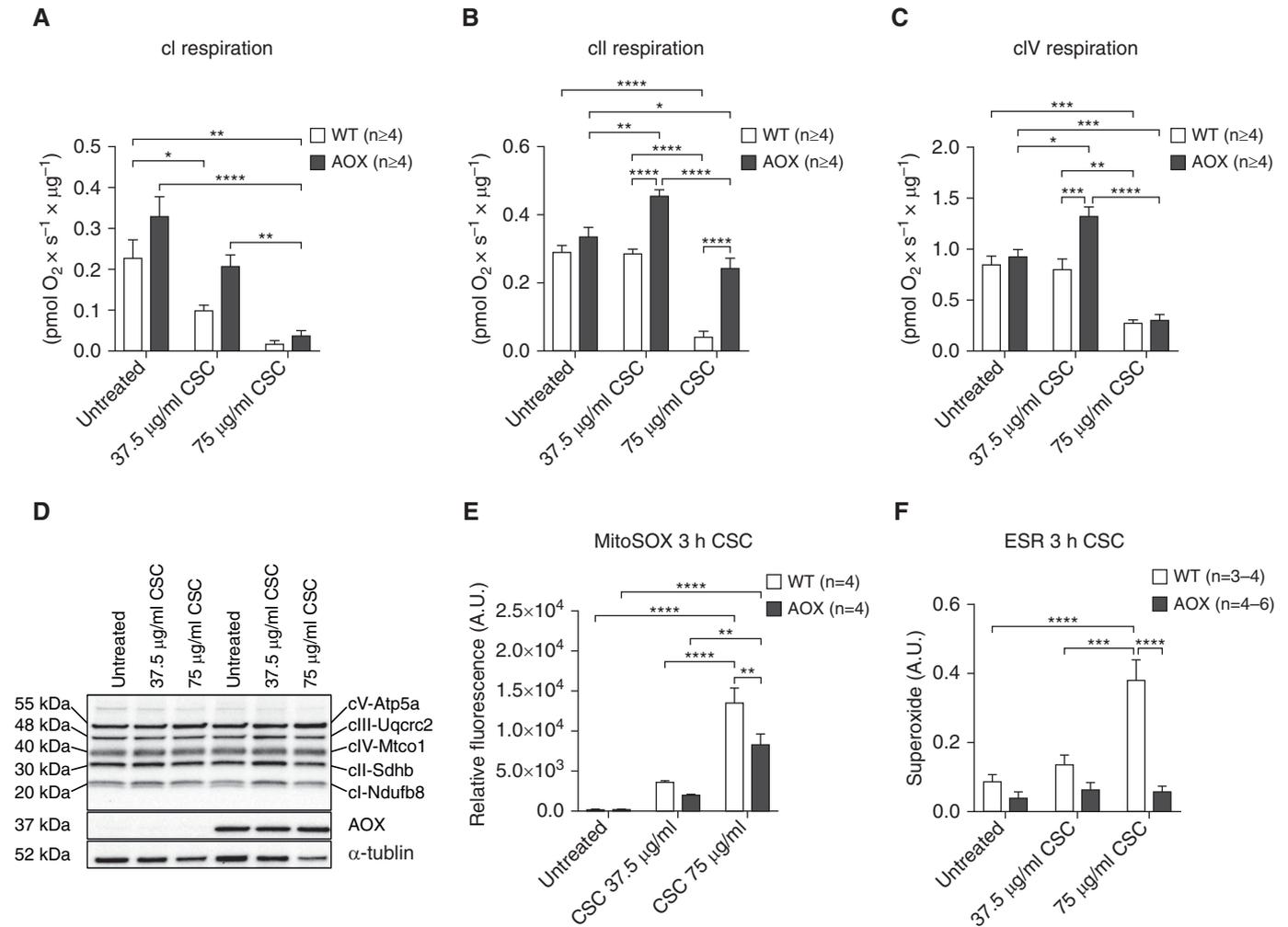
Figure 4. CSC toxicity effect on mitochondrial respiration and reactive oxygen species production in cultured iMEFs. (*A*) Oxygen consumption of permeabilized iMEFs in respiration buffer after culturing in gal media for 48 hours conditioned with CSC as indicated. Rotenone-sensitive oxygen consumption in the presence of complex I (cI) substrates pyruvate, glutamate, and malate plus ADP. (*B*) Antimycin A– plus n-propyl gallate–sensitive oxygen consumption in the presence of succinate (complex II [cII]) plus rotenone. (*C*) Sodium azide–sensitive oxygen consumption in the presence of ascorbate/TMPD (complex IV [cIV]). (*D*) Representative Western blot ($n \geqslant 3$) probed for subunits of the complexes of the mitochondrial OXPHOS system as indicated, with AOX and α-tubulin as the loading control. For entire blots, including molecular-weight markers for cropped Western blot bands, please refer to Figure E6. (*E*) Mitochondrial superoxide production measured using MitoSOX Red in iMEFs grown in glucose media (10 mM) after 3 hours of CSC exposure as indicated. (*F*) Determination of superoxide production using the spin probe CMH (1-hydroxy3-methoxycarbonyl-2,2,5,5-tetramethylpyrrolidine) and subtraction of pSOD (superoxide dismutase)-sensitive signal from total signal [CMH − (CMH + pSOD)] in iMEFs grown in glucose media (10 mM) after 3 hours of CSC exposure as indicated. All data are shown as mean ± SEM; *$P < 0.05$, **$P < 0.005$, ***$P < 0.0005$, and ****$P < 0.0001$ by two-way ANOVA. ESR = electronic spin resonance.

death by necrosis and/or apoptosis (29, 30). It is also of interest that the contents of CS affect membrane fluidity (31, 32). This alone may explain the observed respiratory impairment. More experiments will be needed to elucidate the exact pathomechanism, but the use of AOX provides a powerful route to this end.

A study of this type has intrinsic limitations that complicate translation of the results. For instance, it is well known that the murine lung regenerates much more efficiently

than the adult human lung in response to CS. Here, we used mice on a C57BL/6 genetic background. The advantage of using such mice lies clearly in the comparability of data, as this strain is widely used. Unfortunately, however, C57BL/6 mice are exceptionally well protected against CS (33). Our results may therefore underestimate the protective effect of AOX. Indeed, the changes indicative of the development of emphysema are small, albeit significant, and compatible with previous results obtained using the same smoke

machine and strain (13, 14). Nevertheless, other strains, such as AKR/J, are more susceptible to CS (33) and should be used in follow-up studies. Furthermore, CSC is a well-established surrogate for smoke exposure in cultured cells, but due to the isolation procedure and the constraints of cell culture, smoke and CSC differ significantly in composition. On the other hand, lung fibroblasts, epithelial cells, and macrophages also detect only those CS components that are dissolved in the fluid
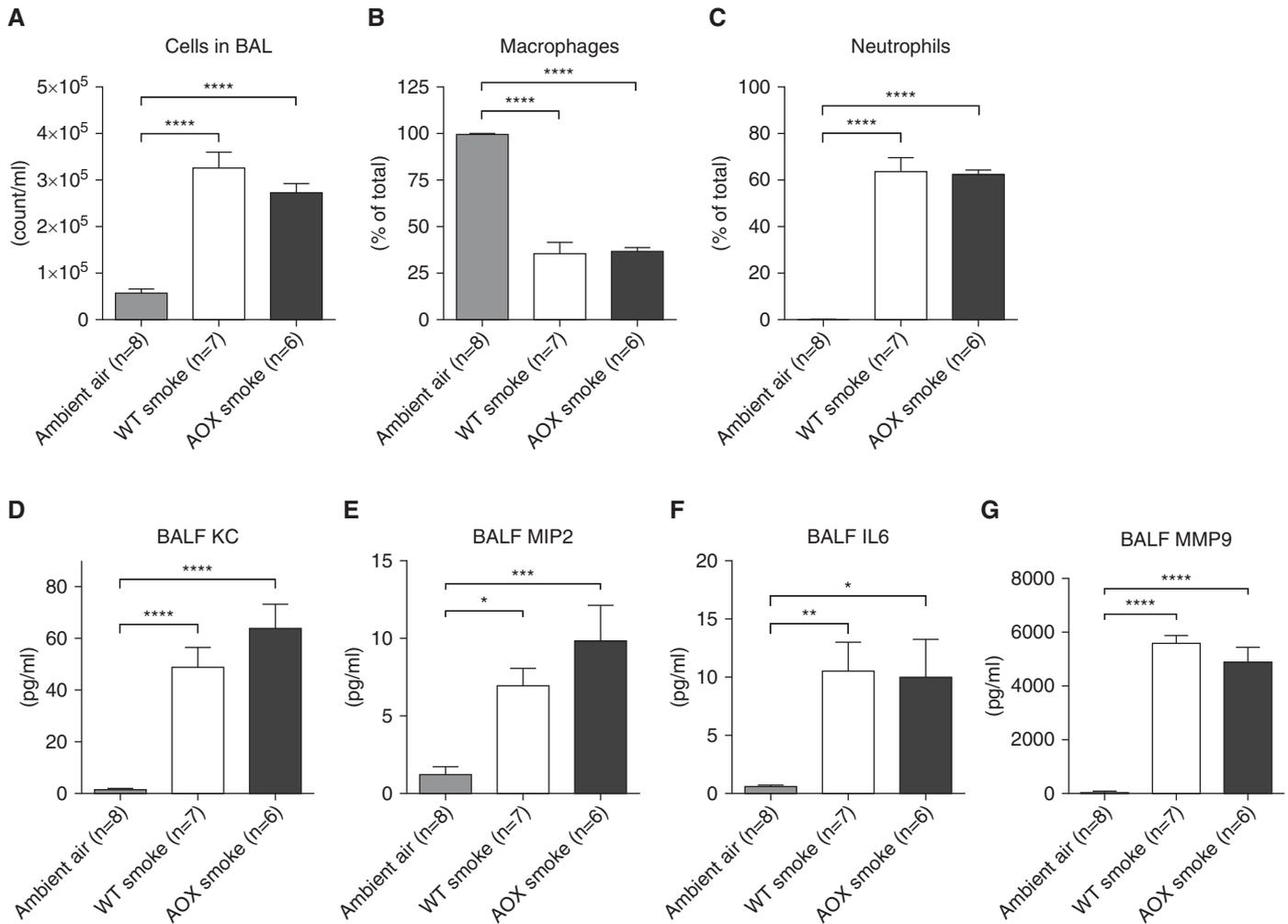
Figure 5. Testing the effect of acute CS exposure and AOX on inflammatory cell infiltration. (*A*) Total number of cells in BAL of WT and AOX mice upon short-term smoke exposure. (*B* and *C*) Macrophages and neutrophils as a percentage of total cells in BAL. (*D*–*G*) Selected inflammatory signals in BAL fluid (BALF). Note that owing to identical behavior and phenotype, the control group in ambient air is composed of WT and AOX mice. All data are shown as mean $\pm$ SEM; *$P < 0.05$, **$P < 0.005$, ***$P < 0.0005$, and ****$P < 0.0001$ by one-way ANOVA. KC = keratinocyte-derived cytokine, CXCL1; MIP2 = macrophage inflammatory protein 2; MMP9 = matrix metalloprotease 9.

lining the airways. Thus, the effects of CSC may actually truly reflect the *in vivo* situation. Finally, although the transgenic expression of AOX undoubtedly protects against cellular and lung maladaptation, deploying AOX in a therapeutic context remains a distant prospect. This will require extensive studies on its delivery, durability, and safety.

The most surprising finding of the current study is that the inflammatory response to acute CS exposure for 3 days was unaffected by AOX. A recent study claimed that macrophages from patients with COPD expressed more enzymes that promote tissue remodeling than healthy control subjects, and macrophages from patients with COPD showed higher expression of M2-related genes while suppressing M1 inflammatory and immune-regulatory

proteins (34). Our findings indicate that mitochondrial respiratory inhibition is not the trigger for the immediate tissue response, even though it is clearly involved in the long-term pathogenic process. This appears to contrast with previous findings that infiltration and activation of macrophages and especially neutrophils correlate with an adverse outcome (35). Importantly, in our model, AOX is expressed ubiquitously (6). Thus, it is not possible to distinguish whether the critical target tissue in which mitochondrial respiratory inhibition leads to indicators of emphysema is the lung epithelium itself, macrophages, or other cells of the immune system (36), or some other tissue entirely. This can only be addressed by the creation of models in which AOX expression is limited to

specific tissues or cell types, which will clearly be the subject of future studies.

In conclusion, expression of AOX attenuates CS-induced lung remodeling and protects cultured fibroblasts from CSC-induced cell death. This is associated with maintenance of respiration and decreased ROS production. Thus, AOX represents an innovative tool to study CS-induced lung diseases and may serve as the basis for lung protection. ■

References

1. Vestbo J, Hurd SS, Agustí AG, Jones PW, Vogelmeier C, Anzueto A, et al. Global strategy for the diagnosis, management, and prevention of chronic obstructive pulmonary disease: GOLD executive summary. *Am J Respir Crit Care Med* 2013;187:347–365.

2. Chung KF, Adcock IM. Multifaceted mechanisms in COPD: inflammation, immunity, and tissue repair and destruction. *Eur Respir J* 2008;31: 1334–1356.

3. Pryor WA, Stone K. Oxidants in cigarette smoke. Radicals, hydrogen peroxide, peroxynitrate, and peroxynitrite. *Ann N Y Acad Sci* 1993; 686:12–27; discussion 27–28.

4. Talhout R, Schulz T, Florek E, van Benthem J, Wester P, Opperhuizen A. Hazardous compounds in tobacco smoke. *Int J Environ Res Public Health* 2011;8:613–628.

5. Bhandari RK, Oda RP, Petrikovics I, Thompson DE, Brenner M, Mahon SB, et al. Cyanide toxicokinetics: the behavior of cyanide, thiocyanate and 2-amino-2-thiazoline-4-carboxylic acid in multiple animal models. *J Anal Toxicol* 2014;38:218–225.

6. Szibor M, Dhandapani PK, Dufour E, Holmström KM, Zhuang Y, Salwig I, et al.; German Mouse Clinic Consortium. Broad AOX expression in a genetically tractable mouse model does not disturb normal physiology. *Dis Model Mech* 2017;10:163–171.

7. El-Khoury R, Dufour E, Rak M, Ramanantsoa N, Grandchamp N, Csaba Z, et al. Alternative oxidase expression in the mouse enables bypassing cytochrome c oxidase blockade and limits mitochondrial ROS overproduction. *PLoS Genet* 2013;9:e1003182.

8. Dry IB, Moore AL, Day DA, Wiskich JT. Regulation of alternative pathway activity in plant mitochondria: nonlinear relationship between electron flux and the redox poise of the quinone pool. *Arch Biochem Biophys* 1989;273:148–157.

9. El-Khoury R, Kemppainen KK, Dufour E, Szibor M, Jacobs HT, Rustin P. Engineering the alternative oxidase gene to better understand and counteract mitochondrial defects: state of the art and perspectives. *Br J Pharmacol* 2014;171:2243–2249.

10. Dassa EP, Dufour E, Goncalves S, Jacobs HT, Rustin P. The alternative oxidase, a tool for compensating cytochrome c oxidase deficiency in human cells. *Physiol Plant* 2009;137:427–434.

11. Mills EL, Kelly B, Logan A, Costa ASH, Varma M, Bryant CE, et al. Succinate dehydrogenase supports metabolic repurposing of mitochondria to drive inflammatory macrophages. *Cell* 2016;167: 457–470.e13.

12. Wolf L, Herr C, Niederstraßer J, Beisswenger C, Bals R. Receptor for advanced glycation endproducts (RAGE) maintains pulmonary structure and regulates the response to cigarette smoke. *PLoS One* 2017;12:e0180092.

13. Voss M, Wolf L, Kamyschnikow A, Wonnenberg B, Honecker A, Herr C, et al. Il-17A contributes to maintenance of pulmonary homeostasis in a murine model of cigarette smoke-induced emphysema. *Am J Physiol Lung Cell Mol Physiol* 2015;309:L188–L195.

14. Herr C, Han G, Li D, Tschernig T, Dinh QT, Beißwenger C, et al. Combined exposure to bacteria and cigarette smoke resembles characteristic phenotypes of human COPD in a murine disease model. *Exp Toxicol Pathol* 2015;67:261–269.

15. Abbondanzo SJ, Gadi I, Stewart CL. Derivation of embryonic stem cell lines. *Methods Enzymol* 1993;225:803–823.

16. Lochmüller H, Johns T, Shoubridge EA. Expression of the E6 and E7 genes of human papillomavirus (HPV16) extends the life span of human myoblasts. *Exp Cell Res* 1999;248:186–193.

17. Giordano L, Deceglie S, d'Adamo P, Valentino ML, La Morgia C, Fracasso F, et al. Cigarette toxicity triggers Leber's hereditary optic neuropathy by affecting mtDNA copy number, oxidative phosphorylation and ROS detoxification pathways. *Cell Death Dis* 2015;6:e2021.

18. Vichai V, Kirtikara K. Sulforhodamine B colorimetric assay for cytotoxicity screening. *Nat Protoc* 2006;1:1112–1116.

19. Kuznetsov AV, Veksler V, Gellerich FN, Saks V, Margreiter R, Kunz WS. Analysis of mitochondrial function in situ in permeabilized muscle fibers, tissues and cells. *Nat Protoc* 2008;3:965–976.

20. Wojtala A, Bonora M, Malinska D, Pinton P, Duszyński J, Wieckowski MR. Methods to monitor ROS production by fluorescence microscopy and fluorometry. *Methods Enzymol* 2014;542:243–262.

21. Sommer N, Hüttemann M, Pak O, Scheibe S, Knoepp F, Sinkler C, et al. Mitochondrial complex IV subunit 4 isoform 2 is essential for acute pulmonary oxygen sensing. *Circ Res* 2017;121:424–438.

22. Robinson BH, Petrova-Benedict R, Buncic JR, Wallace DC. Nonviability of cells with oxidative defects in galactose medium: a screening test for affected patient fibroblasts. *Biochem Med Metab Biol* 1992;48: 122–126.

23. Papaporfyriou A, Loukides S, Kostikas K, Simoes DCM, Papatheodorou G, Konstantellou E, et al. Increased levels of osteopontin in sputum supernatant in patients with COPD. *Chest* 2014;146: 951–958.

24. Thatcher TH, McHugh NA, Egan RW, Chapman RW, Hey JA, Turner CK, et al. Role of CXCR2 in cigarette smoke-induced lung inflammation. *Am J Physiol Lung Cell Mol Physiol* 2005;289: L322–L328.

25. Zhang XW, Liu Q, Wang Y, Thorlacius H. CXC chemokines, MIP-2 and KC, induce P-selectin-dependent neutrophil rolling and extravascular migration in vivo. *Br J Pharmacol* 2001;133:413–421.

26. Deshmukh HS, Shaver C, Case LM, Dietsch M, Wesselkamper SC, Hardie WD, et al. Acrolein-activated matrix metalloproteinase 9 contributes to persistent mucin production. *Am J Respir Cell Mol Biol* 2008;38:446–454.

27. Ferry G, Lonchampt M, Pennel L, de Nanteuil G, Canet E, Tucker GC. Activation of MMP-9 by neutrophil elastase in an in vivo model of acute lung injury. *FEBS Lett* 1997;402:111–115.

28. Mercer PF, Shute JK, Bhowmik A, Donaldson GC, Wedzicha JA, Warner JA. MMP-9, TIMP-1 and inflammatory cells in sputum from COPD patients during exacerbation. *Respir Res* 2005;6:151.

29. Esakky P, Hansen DA, Drury AM, Cusumano A, Moley KH. Cigarette smoke-induced cell death of a spermatocyte cell line can be prevented by inactivating the Aryl hydrocarbon receptor. *Cell Death Discov* 2015;1:15050.

30. Messner B, Frotschnig S, Steinacher-Nigisch A, Winter B, Eichmair E, Gebetsberger J, et al. Apoptosis and necrosis: two different outcomes of cigarette smoke condensate-induced endothelial cell death. *Cell Death Dis* 2012;3:e424.

31. Hannan SE, Harris JO, Sheridan NP, Patel JM. Cigarette smoke alters plasma membrane fluidity of rat alveolar macrophages. *Am Rev Respir Dis* 1989;140:1668–1673.

32. Collin A, Hardonnière K, Chevanne M, Vuillemin J, Podechard N, Burel A, et al. Cooperative interaction of benzo[a]pyrene and ethanol on plasma membrane remodeling is responsible for enhanced oxidative stress and cell death in primary rat hepatocytes. *Free Radic Biol Med* 2014;72:11–22.

33. Guerassimov A, Hoshino Y, Takubo Y, Turcotte A, Yamamoto M, Ghezzo H, et al. The development of emphysema in cigarette smoke-exposed mice is strain dependent. *Am J Respir Crit Care Med* 2004; 170:974–980.

34. Shaykhiev R, Krause A, Salit J, Strulovici-Barel Y, Harvey B-G, O'Connor TP, et al. Smoking-dependent reprogramming of alveolar macrophage polarization: implication for pathogenesis of chronic obstructive pulmonary disease. *J Immunol* 2009;183:2867–2883.

35. Barnes PJ. Inflammatory mechanisms in patients with chronic obstructive pulmonary disease. *J Allergy Clin Immunol* 2016;138: 16–27.

36. Seimetz M, Parajuli N, Pichl A, Veit F, Kwapiszewska G, Weisel FC, et al. Inducible NOS inhibition reverses tobacco-smoke-induced emphysema and pulmonary hypertension in mice. *Cell* 2011;147: 293–305.